

Damping properties and morphology of polyurethane/vinyl ester resin interpenetrating polymer network

Chuan-Li Qin^{a,b}, Wei-Min Cai^{a,b,*}, Jun Cai^b, Dong-Yan Tang^c, Ju-Sheng Zhang^c, Mei Qin^d

^a Department of Environmental Science and Engineering, Harbin Institute of Technology, Harbin 150001, PR China

^b Department of Environmental Science and Engineering, Shanghai Jiaotong University, Shanghai 200030, PR China

^c Department of Applied Chemistry, Harbin Institute of Technology, Harbin 150001, PR China

^d School of Chemical and Environmental Engineering, Harbin University of Science and Technology, Harbin 150080, PR China

Received 25 September 2003; received in revised form 4 November 2003; accepted 28 January 2004

Abstract

A series of polyurethane/vinyl ester resin simultaneous and gradient interpenetrating polymer networks (PU/VER IPN and gradient IPN), cured at room temperature, were synthesized by introducing acrylic esters as VER's comonomers. The effects of thermodynamic factor, kinetic factor, component ratio and gradient techniques on their damping properties were studied by DMA. It was found that the damping properties of general PU/VER (St) IPN with styrene (St) as VER's comonomer are improved by introducing acrylic esters instead of St. When the relative polymerization rates of the networks are close, 80:20, 70:30 and 60:40 PU/VER (BMA) IPNs with butyl methacrylate (BMA) as VER's comonomer have excellent damping properties. The gradient IPN with better damping properties than simultaneous IPNs was obtained by adjusting the gradient techniques. The $\tan \delta$ values of the gradient IPN with the time interval of 3 h and the component ratios of 50:50–60:40–70:30 are higher than 0.3 from -57°C to higher than 90°C , and its $\tan \delta$ values are higher than 0.5 from -36 to 54°C . The results of EDX revealed that the gradient structure is formed in transition regions of gradient IPN. The results detected by TEM and AFM showed that the phase ranges of PU/VER (BMA) IPNs and gradient IPN obtained are both in nanometer scale. Furthermore, the relationship of microstructure and damping properties was studied.

© 2004 Elsevier B.V. All rights reserved.

Keywords: Polyurethane; Vinyl ester resin; Gradient IPN; Damping properties

1. Introduction

Material damping is one of the most effective solutions to the problem of vibration and noise. Viscoelastic polymers as damping materials have attracted many researchers in recent years because of their high damping values around the glass transition temperature (T_g) [1,2]. But the useful damping temperature range of a homopolymer usually covers 20 – 30°C for acoustical frequency ranging from 20 to $20\,000$ Hz, which is rather narrow for practical applications. In fact, the $\tan \delta$ values of good damping materials are higher than 0.3 for a temperature range of at least 60°C [3]. In order to improve the damping capabilities of polymers, many techniques, such as polymer blends, copolymers, and interpenetrating polymer networks (IPNs or IPN) have been employed. Among them, IPN, a novel type of polymer al-

loys consisting of two or more crosslinked polymers held together by physical entanglement, has been the promising technique of preparing materials with broad T_g ranges and excellent damping performances because of mutual entanglement, forced compatibility, synergism of the networks and cellular, dual-phase continuous microstructure [4,5].

Gradient IPN is mixture of crosslinked polymers in which the concentration of one network changes across the section of a sample. So, it may be regarded as a combination of an infinite number of layers of IPN, whose compositions and properties vary gradually from the surface to the core of the sample. As a result, the properties of the system differ from those of both individual network and IPN prepared by the traditional method. It was shown that gradient IPN had a broad maximum of mechanical loss tangent ($\tan \delta$) spanning a temperature range from 273 to 373 K [6]. Gradient IPN is obtained by the method of sequential curing, so it cannot be prepared by traditional method in the system cured at room temperature in which the process of diffusion and curing of the monomers forming the second network is simultaneous.

* Corresponding author. Tel.: +86-451-8641-3710;

fax: +86-451-8641-3710.

E-mail address: chuanliqin@sohu.com (W.-M. Cai).

In the previous work [7], the polyurethane/poly(methyl methacrylate) gradient IPN cured at room temperature was obtained by casting the mixture of different component ratios in a mold at various times and the detected results showed that the gradient IPN revealed many sublevel transitions. In this paper, a series of polyurethane/vinyl ester resin (PU/VER) simultaneous and gradient IPNs were synthesized by this method. For PU/VER IPN, a great deal of research has been concentrated on their synthesis, morphology and mechanical properties, but seldom on their damping properties [8,9]. And there is still few literature about damping properties of gradient IPN [6]. Generally, styrene (St) is VER's comonomer, which may result in the poor compatibility and damping properties of PU/VER (St) IPN (St is VER's comonomer) because PU and polystyrene (PSt) are incompatible thermodynamically [10]. Wang et al. [11] improved the compatibility and mechanical properties of PU/VER IPN by introducing methyl methacrylate (MMA) as grafted VER's comonomer. In this paper, in order to improve the compatibility and damping properties of PU/VER IPN, different acrylic esters were introduced into VER's comonomer system. The effects of thermodynamic factor, kinetic factor, component ratio of IPN and techniques of gradient IPN on their damping properties were studied. Furthermore, the relationship of microstructure and damping properties was studied.

2. Experimental

2.1. Materials

PU prepolymer was prepared in our laboratory [12]. Epoxy acrylate was supplied by Shanghai Synthetic Resin Plant. Butyl methacrylate (BMA), styrene, methyl methacrylate, ethyl acrylate (EA), benzoyl peroxide (BPO), 1,4-butylene glycol(1,4-BD), *N,N'*-dimethylaniline (DMA), trimethylol propane (TMP), stannous octoate (T-9), ethyl acetate (EAc) were chemically pure and obtained from various suppliers.

TMP was dried at 383 K under vacuum for 3 h. Inhibitors were removed from St, EA, MMA and BMA. EAc was dehydrated by reduced pressure distillation.

2.2. Preparation of simultaneous and gradient IPN samples

To prepare simultaneous IPNs, calculated amount of TMP as PU crosslinker was dissolved in dehydrated EAc. Then 1,4-BD as PU chain-extender, epoxy acrylate, acrylic ester (or St), PU prepolymer, BPO-DMA as redox initiators and T-9 as catalyst for PU were added. After the mixture was thoroughly stirred and degassed under vacuum for 5–10 min, a yellow and transparent sample was prepared by curing it at room temperature in a mold. A series of IPNs in this way were synthesized by varying VER's comonomers, the amounts of catalyst for PU and initiators for VER, the com-

ponent ratios of PU and VER in the system. The gradient IPNs were obtained by casting the mixture of different component ratios in a mold at various times during the curing process of IPN.

2.3. Measurements

Dynamic mechanical analysis (DMA) was carried out on a Metravib MAK-04 Viscoanalyser over a temperature range from -75 to 100 °C at a heating rate of 3 °C min^{-1} at 11 Hz. The samples were rectangular bars (2.0 cm \times 1.5 cm \times 0.2 cm).

Transmission electron microscope (TEM) observations were carried out using a JEM 1200-EX apparatus type. The samples were cut into ultra-thin section about 100 nm thickness with an freezing superthin microtome in liquid nitrogen and stained with 2% OsO₄ vapor for 48 h.

Atomic force microscopy (AFM) imaging was performed on microtomed surfaces with a digital instrument Nanoscope III scanning probe microscope with multimode head and J-scanner. The tapping mode was used at ambient conditions. Commercial Si probes were chosen. The resonance frequencies of these probes were in the 300 kHz range. Height and phase images were recorded, simultaneously.

Energy dispersive X-ray (EDX) analysis was done using a Oxford ISIS-300 spectrometer coupled to a JEOL JXA-840 scanning electron microscope on the cross-section of a sample. The sample was prepared by fracturing it in liquid nitrogen in the direction of thickness and applying a conducting gold coating in order to reduce the charging effect.

3. Results and discussion

3.1. The influence of VER's comonomers

Fig. 1 shows the plots of $\tan \delta$ versus temperature of 60:40 PU/VER IPNs (the component ratio of PU and VER

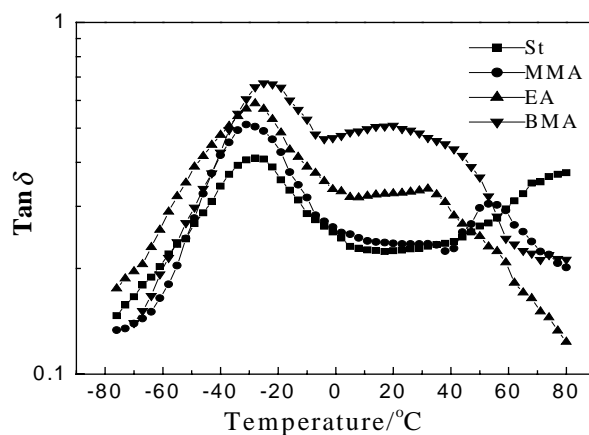


Fig. 1. DMA curves of 60:40 PU/VER IPNs with different VER's comonomers.

by weight is 60:40) with different VER's comonomers. As shown in Fig. 1, the damping properties of PU/VER IPNs with acrylic esters as VER's comonomers are better than those of PU/VER (St) IPN which shows that the "valley" between the two peaks is more pronounced. The damping properties of PU/VER (EA) IPN are better than those of PU/VER (MMA) IPN for a broad temperature range. PU/VER (BMA) IPN shows the best damping properties due to the fact that the IPN has broad and high damping platform compared with two separate peaks and low $\tan \delta$ values between peaks of the others.

The results can be attributed to the fact that the damping properties of IPN are mainly affected by the compatibility between the networks. The compatibility of PSt and PU is poor because the solubility parameter difference ($\Delta\delta$) of PSt ($1.81 \times 10^4 \text{ J}^{1/2} \text{ m}^{2/3}$) and PU ($2.04 \times 10^4 \text{ J}^{1/2} \text{ m}^{2/3}$) is large [13]. Despite larger $\Delta\delta$ of PBMA ($1.78 \times 10^4 \text{ J}^{1/2} \text{ m}^{2/3}$) and PU compared with that of PSt and PU, PBMA has polar carboxy and the compatibility of PU/VER(BMA) IPN can be improved due to hydrogen bonds between polar carboxy and amino of PU. Furthermore, T_g of PBMA is located between those of PU and epoxy acrylate of VER, so it can effectively link their T_g 's. The $\Delta\delta$ of PEA ($1.90 \times 10^4 \text{ J}^{1/2} \text{ m}^{2/3}$), PMMA ($1.90 \times 10^4 \text{ J}^{1/2} \text{ m}^{2/3}$) and PU is smaller. So on the one hand, the compatibility of PU/VER (EA) IPN, PU/VER (MMA) IPN, PU/VER (BMA) IPN is better than that of PU/VER (St) IPN.

On the other hand, the results are attributable to the effects of different molecular structure on damping properties of IPN. The PU/VER IPNs which have acrylic esters as VER's comonomers have more flexible ester groups instead of rigid phenyl of PU/VER (St) IPN in the VER's comonomer system and they have greater friction force during the movement of segments, that contributes to better damping properties. Among them, as proved by Huang and Li [4], methyl ester groups of PU/VER (MMA) IPN, because of their stiffness and volume effect, retard the internal rotation of the main chain and weaken intermolecular friction. However, PU/VER (EA) IPN and PU/VER (BMA) IPN have ethyl ester and butyl ester groups with relatively lower potential barrier and more mobility, given that the side ester groups cause the distance between the molecules to increase, which can offset the volume effect of the bulky groups, and they have better damping properties than PU/VER (MMA) IPN. PU/VER (BMA) IPN shows best damping properties because of greatest butyl ester groups.

3.2. The influence of the relative polymerization rates

When the thermodynamic factor (the type of components) is determined, kinetics is the main factor affecting the compatibility and damping properties of IPN. Fig. 2 shows DMA curves of 60:40 PU/VER (BMA) IPNs with different amounts of T-9 (the amount of BPO is 0.67 wt.% of VER). The amount of T-9 affects damping properties of IPN because of its influence on relative polymerization

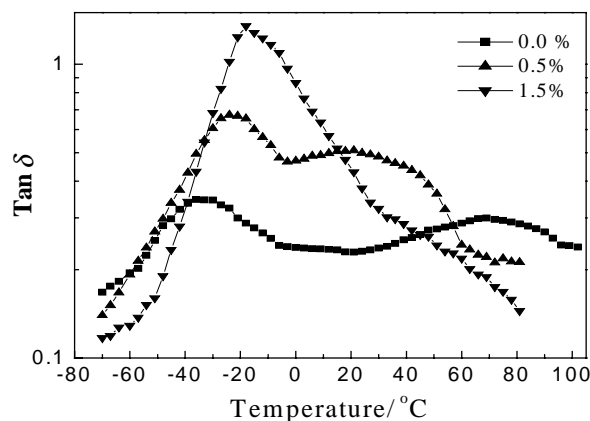


Fig. 2. DMA curves of 60:40 PU/VER (BMA) IPNs with different amounts of T-9.

rates of the networks. The IPN with 0.5 wt.% T-9 shows a broad damping plateau and good damping properties, which is due to the fact that the relative polymerization rates are close which has been borne out by other paper [14]. The IPN without T-9 shows obvious phase separation and poor damping properties, which is perhaps due to the fact that the relative polymerization rates are greatly different. When the amount of T-9 is 1.5 wt.% of PU, the height of the low-temperature damping peak obviously increases, whereas the damping peak is narrow and damping properties are poor, which is due to the fact that the network of PU is formed quickly, so the monomers of VER are "trapped" in the network of PU and it prevents the appropriate phase separation of VER and PU phases when the polymerization of VER is eventually completed [15].

Fig. 3 shows plots of $\tan \delta$ versus temperature of 70:30 PU/VER (BMA) IPNs with different amounts of T-9 and BPO. As shown in Fig. 3, when the amount of BPO is 0.67 wt.% of VER, with the increase of T-9, the damping peak becomes narrow and damping properties become poor which is consistent with the conclusion in Fig. 2. The IPN with 0.5 wt.% T-9 and 0.67 wt.% BPO shows a broad damp-

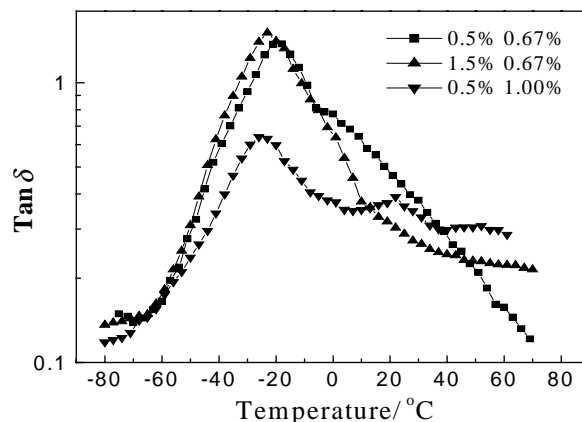


Fig. 3. DMA curves of 70:30 PU/VER (BMA) IPNs with different amounts of T-9 and BPO.

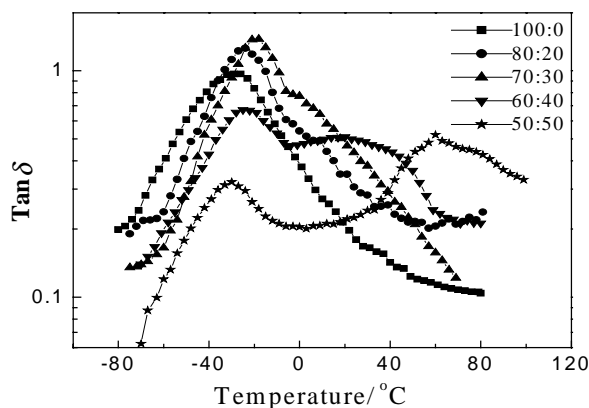


Fig. 4. DMA curves of PU/VER (BMA) IPNs with component ratios from 100:0 to 50:50.

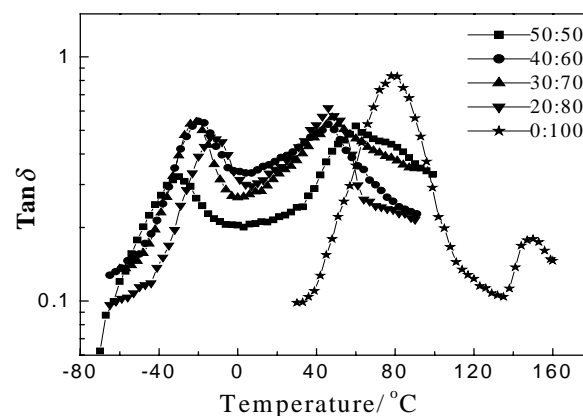


Fig. 5. DMA curves of PU/VER (BMA) IPNs with component ratios from 50:50 to 0:100.

ing peak and high $\tan \delta$ values. When T-9 is constant, with the increase of BPO, the IPN shows two low and separate damping peaks, which is due to the fact that the amount of BPO also directly affects relative polymerization rates. The step polymerization of PU begins earlier than the radical polymerization of VER. The polymerization rate of VER network increases with the increase of BPO, but PU network which has become continue phase is not affected greatly (higher damping peak of PU shows that PU phase is continue). The entropy (ΔS) in the system decreases, and the Gibbs free energy (ΔG) increases, which results in phase separation and poor damping properties.

3.3. The influence of component ratios

Figs. 4 and 5 and Table 1 show DMA curves and data of PU/VER (BMA) IPNs with different component ratios (the amounts of BPO and T-9 are respectively 0.67 wt.% of VER and 0.5 wt.% of PU). As shown, the component ratio is also a main factor which affects the damping properties of IPN. Although synthesized PU has a relative broad damping peak by choosing materials with certain

structure, the T_g range is in low-temperature and VER has a narrow high-temperature damping peak. They cannot meet the requirement of practical applications. The 80:20 and 70:30 IPNs have good damping properties due to the fact that two peaks, corresponding to the T_g 's of pure polymers, nearly form a peak which shows considerable entanglement at molecular level formed in the networks, and their $\tan \delta$ values are higher than 0.3 for a temperature range of 78 and 84 °C, respectively. The damping properties of the IPNs with the component ratios from 50:50 to 30:70 are poor due to two obvious damping peaks and low $\tan \delta$ values between them. The 60:40 IPN has a single broad damping platform and its $\tan \delta$ values are higher than 0.3 for a temperature range of near 100 °C, which shows that the IPN has best damping properties.

According to $\tan \delta$ values and T_g ranges in Table 1 and DMA curves in Figs. 4 and 5, when the component ratios are 80:20, 70:30 and 60:40, $\tan \delta$ values of the IPNs are higher than 0.3 for a temperature range of at least near 80 °C, and they are excellent damping materials with a broad effective damping temperature range.

Table 1

DMA data of PU/VER (BMA) simultaneous and gradient IPNs with different component ratios

PU/VER (wt.%)	Temperature range (°C)		$\tan \delta$ at 24 °C
	$\tan \delta > 0.3$	$\tan \delta > 0.5$	
100:0	-65 to 4	-53 to 8	0.1795
80:20	-54 to 24	-45 to 3	0.3061
70:30	-48 to 36	-42 to 18	0.4346
60:40	-46 to 53	-34 to 10	0.4928
50:50	-33 to 27, 42–99	–	0.2245
40:60	-32 to 67	-23 to 17, 46–49	0.3946
30:70	-33 to 9, 18 to >90	-24 to 21, 45–54	0.3459
20:80	-23 to 1, 10–58	37–52	0.3761
0:100	60–96	66–90	–
40:60–60:40–80:20	-41 to >90	31–49	0.4792
40:60–50:50–60:40	-35 to 55	22–37	0.5111
50:50–60:40–70:30	-57 to >90	-36 to 54	0.6253

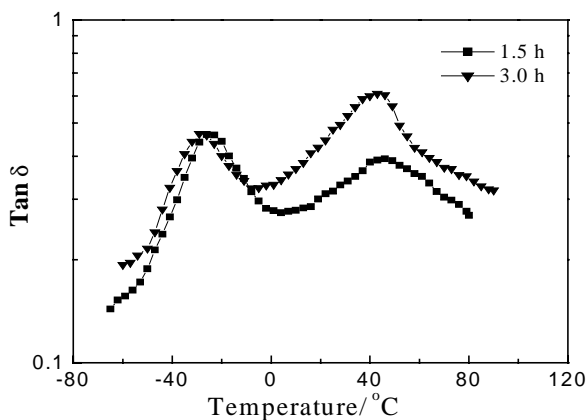


Fig. 6. DMA curves of gradient IPNs with different time intervals of coating.

3.4. The influence of gradient techniques

3.4.1. The influence of the time intervals

Fig. 6 compares the damping properties of gradient IPNs with different time intervals of coating and fixed component ratios of 40:60–60:40–80:20. The gradient IPN with the time interval of 1.5 h when the mixture is just immobile has two separate and low damping peaks, which indicates poor damping properties. It might be due to the fact that the time interval is short and all the layers might nearly mix together. The gradient IPN with the time interval of 3 h when the mixture is just at gelation has two high damping peaks and relative better damping properties because the gradient IPN with longer time interval has different T_g ranges in every layer and the T_g ranges can be linked up and broaden because of the partially gradient structure of transition regions between the layers which will be proved in following

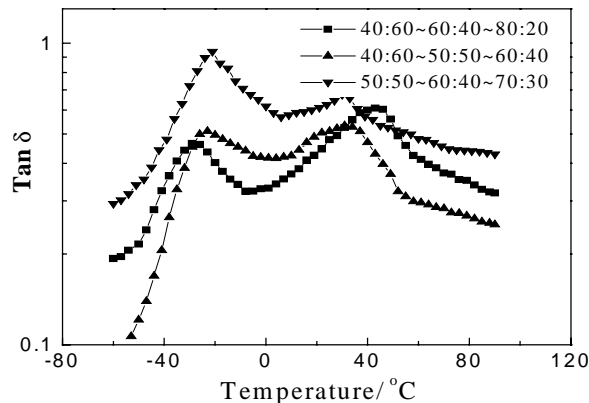


Fig. 7. DMA curves of gradient IPNs with different intervals of component ratios.

EDX analysis. But the damping properties of the gradient IPN are poor from -20 to 20 °C. It might be solved by adjusting component ratios.

3.4.2. The influence of the component ratios

Fig. 7 shows plots of $\tan \delta$ versus temperature of gradient IPNs with different component ratios (the fixed time interval of coating is 3 h). DMA data of gradient IPN are also shown in Table 1. The gradient IPN with the component ratios of 40:60–60:40–80:20 has two separate damping peaks and the $\tan \delta$ values between peaks are low which indicates that T_g ranges are not linked up effectively by the gradient techniques. When the component ratios are 50:50–60:40–70:30 and 40:60–50:50–60:40, the “valleys” between peaks vanish and broad damping plateaus with high $\tan \delta$ values emerge. The broad maximum of the gradient IPN between the T_g s of pure polymers is the result of superposition of a great number of relaxation maxima in the layer and transition regions be-

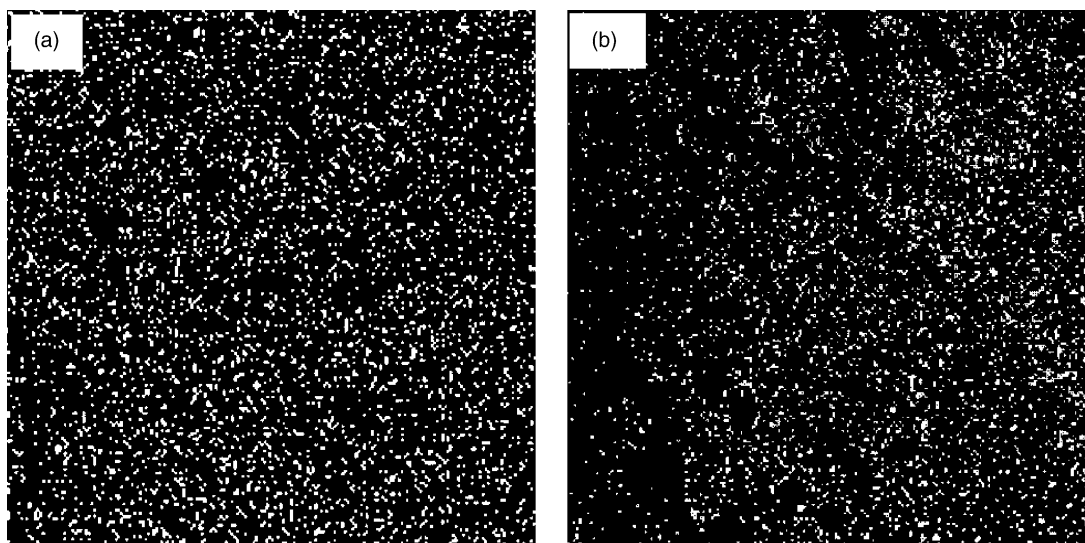


Fig. 8. The surface constitution scan of element N on the cross-section of gradient IPN with the component ratios of 40:60–60:40–80:20 (a) in the layer and (b) in the transition region.

tween layers with progressively varying compositions which has been concluded by Lipatov and Karabanova [6]. As shown in Table 1, the gradient IPN with the component ratios of 50:50–60:40–70:30 has broader T_g range and better damping properties compared with simultaneous IPNs because its $\tan \delta$ values are higher than 0.3 from -57°C to higher than 90°C and $\tan \delta$ values are higher than 0.5 from -36 to 54°C . It shows that the gradient structure of a composite polymeric material indeed brings about an extension of T_g range which realizes the design strategy of gradient IPN. This opens up broad possibilities for manufacture of promising noise and vibration damping materials by this method.

3.5. EDX analysis

In order to verify the gradient structure of the gradient IPN, EDX analysis that examines element distribution is

done. Because the N concentration of PU/VER IPN can indicate the content of PU, N distribution on the cross-section can reflect the distribution of PU. Fig. 8 shows N distribution of the gradient IPN with the time interval of 3 h in the layer and in the transition region between layers. The white spots represent the element of N. As shown in Fig. 8, the element of N is homogeneously distributed in the layer, while the N distribution in the transition region varies gradually from one layer to another layer. The phenomenon is attributable to the fact that the gradient IPN has the fixed component ratio in the layer and partial diffusion between layers by controlling the time interval of coating. On the one hand, the EDX analysis gives clear evidence that in the layer the composition is invariable, whereas the gradient structure exists between layers. On the other hand, because of different component ratios of gradient IPN in different layers, its macrostructure is also gradient. The gra-

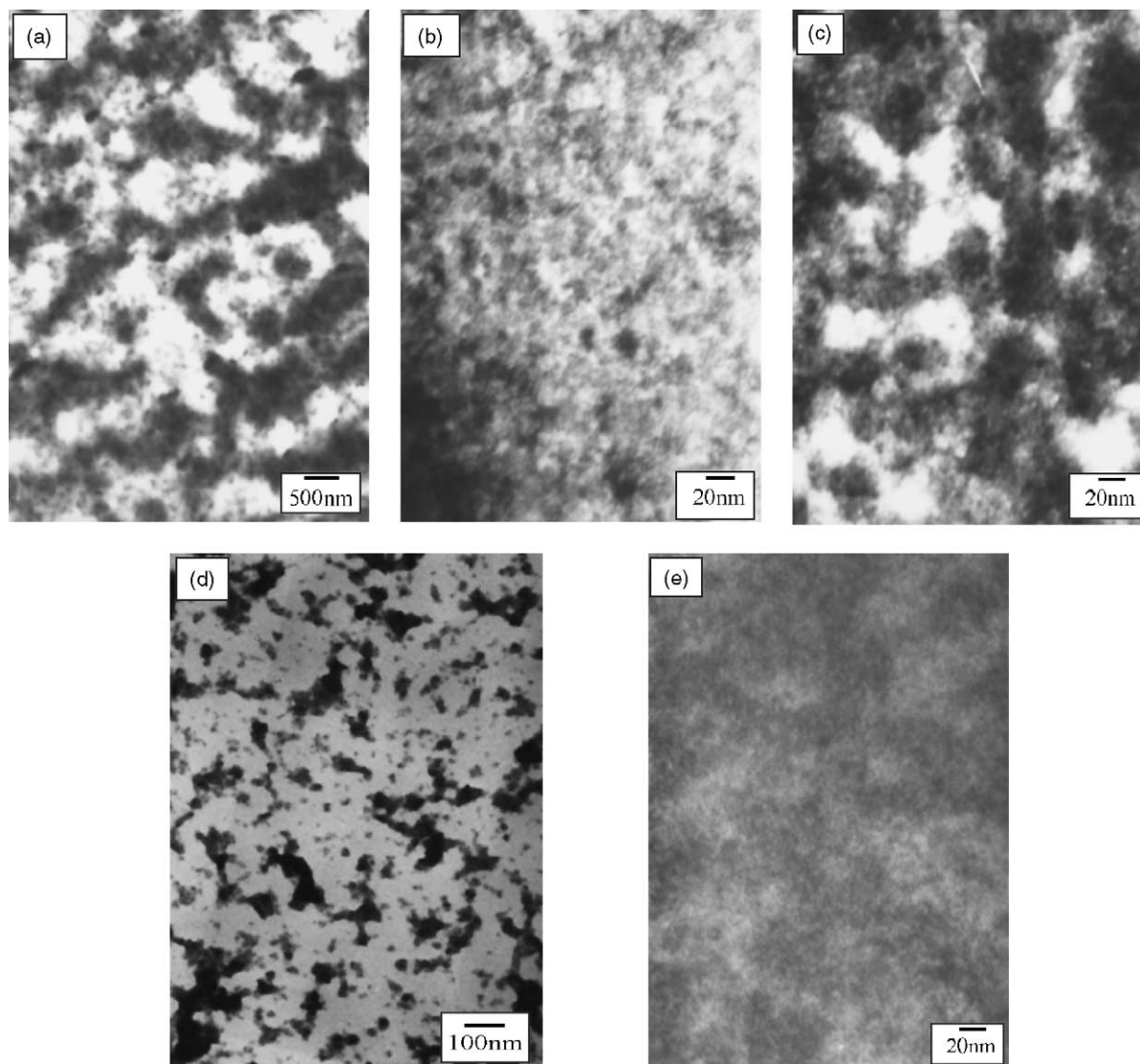


Fig. 9. TEM images of (a) 60:40 PU/VER (St) IPN, (b) 60:40 PU/VER (BMA) IPN, (c) 70:30 PU/VER (BMA) IPN, (d) 50:50 PU/VER (BMA) IPN and (e) the transition region of gradient IPN with the component ratios of 50:50–60:40–70:30.

dient structure contributes to the improvement of damping properties.

3.6. Morphology measurements

TEM images of PU/VER IPNs and gradient IPN are displayed in Fig. 9. The PU phase shows stained by OsO₄. PU/VER (BMA) IPNs are heterogeneous with phase domain sizes ranging from less than 20 nm (Fig. 9(b) and (e)), 20–50 nm (Fig. 9(c)) to 50–100 nm (Fig. 9(d)), which show finer phase domains than PU/VER (St) IPN (Fig. 9(a)) with domain sizes of 200–500 nm. The images provide more direct evidence that the compatibility of PU/VER (St) IPN is improved by introducing BMA instead of St and 60:40 PU/VER (BMA) IPN and gradient IPN have greatest degree of interpenetration.

Because of continuous PU phase and large phase domain sizes of PU/VER (St) IPN, two separate damping peaks with

higher peak of PU appear in its DMA curve. The appearance of more continuous PU phase and small phase domain sizes in (Fig. 9(c)) determines the 70:30 IPN has an obvious damping peak of PU. For 50:50 PU/VER (BMA) IPN, the phase inversion starts and the VER phase becomes the more continuous phase because of the changing of component ratios, so two separate damping peaks with higher peak of VER appear. The morphology of the dual-phase continuity of 60:40 PU/VER (BMA) IPN suggests that the relative polymerization rates of the two networks are approximately same since the network formed firstly tends to be the more continuous one and the morphology of dual-phase continuity determines a damping plateau with approximately same height. It should be mentioned that Fig. 9(e) is the TEM image of the gradient IPN in the transition region between layers and the microstructure of every layer is respectively similar to that of Fig. 9(b)–(d). In these studies, the gradient IPN has the smallest domains in the transition region be-

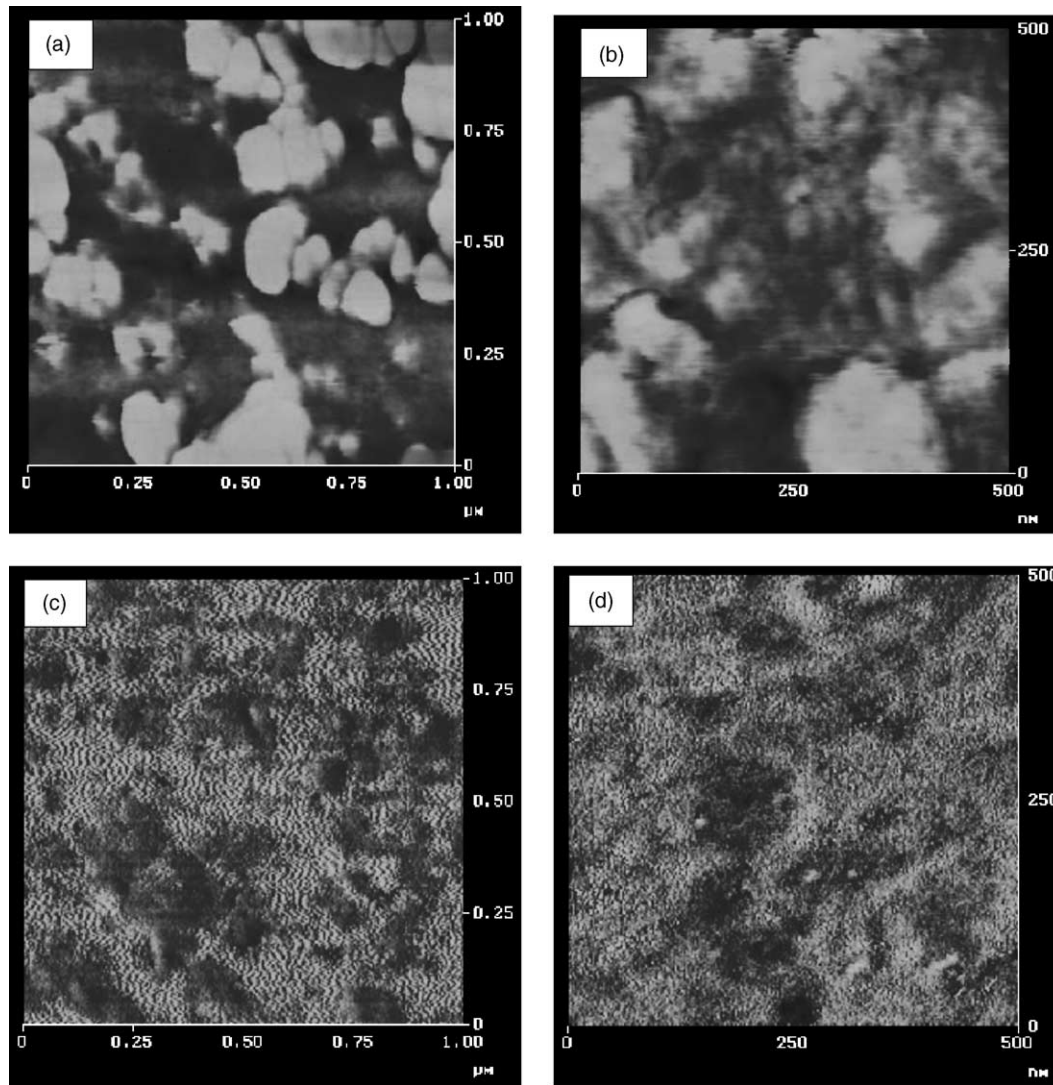


Fig. 10. AFM phase images of (a) 70:30 PU/VER IPN (1 $\mu\text{m} \times 1 \mu\text{m}$), (b) 70:30 PU/VER IPN (500 nm \times 500 nm), (c) 50:50 PU/VER IPN (1 $\mu\text{m} \times 1 \mu\text{m}$) and (d) 50:50 PU/VER IPN (500 nm \times 500 nm).

cause of diffusion and a large number of transitional regions among the phases, so it has the best damping properties with broadest effective damping temperature range. TEM images support the results of DMA.

AFM with tapping mode can also observe microstructure of materials using the principle that phase lag is directly related to the elastic modulus of materials. The modulus difference between PU and VER is large enough to provide good contrast in AFM phase images. Fig. 10 shows AFM images of 70:30 and 50:50 PU/VER (BMA) IPNs. The bright phase is the VER phase with higher modulus and the darker phase is the PU phase with lower modulus. For 70:30 IPN, although VER phase is dispersed in continuous PU phase, obvious gradient distribution emerges in the interface with transition color and the dispersed VER phase is also linked through fine structure but less continuous compared with PU phase. For 50:50 IPN, the larger VER phase sizes and sharper phase boundaries emerge and VER phase becomes continuous. The dispersed PU phase is also linked, but the continuous degree of dispersed phase is lower than that of 70:30 IPN and obvious gradient contribution does not emerge. The results of AFM indicate that the phase ranges of PU/VER (BMA) IPNs obtained are in nanometer scale and the compatibility of 70:30 IPN is better than that of 50:50 IPN, which are in agreement with those of TEM.

4. Conclusions

The thermodynamic factor, that is VER's comonomers in this paper, has great influence on damping properties of PU/VER IPN. The damping properties of general PU/VER (St) IPN are improved by introducing acrylic esters as VER's comonomers. PU/VER (BMA) IPNs with long butyl ester groups show best damping properties.

The amounts of catalyst for PU and initiators for VER and the component ratios also affect the damping properties of IPN. When the amounts of BPO and T-9 are respectively 0.67 wt.% of VER and 0.5 wt.% of PU, 80:20, 70:30 and 60:40 PU/VER (BMA) IPNs have the $\tan \delta$ values of higher than 0.3 in the temperature range of at least near 80 °C and they are excellent damping materials.

The damping temperature range is further broadened by controlling the techniques of gradient IPN. When the time

interval of coating is 3 h, $\tan \delta$ values of the gradient IPN with the component ratios of 50:50–60:40–70:30 are higher than 0.3 from –57 °C to higher than 90 °C and $\tan \delta$ values are higher than 0.5 from –36 to 54 °C. It has better damping properties than simultaneous IPNs due to the gradient structure revealed by the results of EDX. This opens up broad possibilities for manufacture of promising noise and vibration damping materials by gradient techniques.

The different microstructure of IPN determines their different damping properties. PU/VER (BMA) IPNs prepared have the domains of nanometer scale and the gradient IPN has the smallest domains because of a large number of transitional regions among the phases in the transition region which determines its best damping properties.

Acknowledgements

The authors gratefully acknowledge the Nature Science Foundation Committee of Heilongjiang Province for financial support (Grant no. B00-10).

References

- [1] V.R. Buravalla, C. Remillat, J.A. Rongong, G.R. Tomlinson, *Smart Mater. Bull.* 8 (2001) 10.
- [2] P.H. Sung, C.Y. Lin, *Eur. Polym. J.* 33 (1997) 231.
- [3] Y.Q. Yang, M. Du, Q. Zheng, *J. Found. Mater.* 33 (2002) 234.
- [4] G.S. Huang, Q. Li, *J. Appl. Polym. Sci.* 85 (2002) 545.
- [5] Y.C. Chern, S.M. Tseng, K.H. Hsieh, *J. Appl. Polym. Sci.* 74 (1999) 328.
- [6] Y.S. Lipatov, L.V. Karabanova, *J. Mater. Sci.* 30 (1995) 2475.
- [7] D.Y. Tang, L.S. Qiang, Z. Jin, W.M. Cai, *J. Appl. Polym. Sci.* 84 (2002) 709.
- [8] G.Y. Wang, Y.L. Wang, C.P. Hu, *Eur. Polym. J.* 36 (2000) 735.
- [9] Y.J. Wan, Y. Gu, M.L. Xie, Y.Q. Ou, X.P. Liu, W. Lu, J.H. Wang, *J. Funct. Polym.* 13 (2000) 81.
- [10] S.C. Kim, D. Klemperer, L.H. Frisch, *Polym. Eng. Sci.* 15 (1975) 339.
- [11] G.Y. Wang, C.P. Hu, *Acta Chim. Sinica* 59 (2001) 2012.
- [12] C.L. Qin, J.S. Zhang, D.Y. Tang, W.M. Cai, *J. Nat. Sci. Heilongjiang Univ.* 20 (2003) 96.
- [13] J.B. Yan, Y.K. Zhang, *Polymer Handbook of Physical Chemistry*, vol. 1, Petrochemistry Press, China, 1995, p. 235.
- [14] C.L. Qin, J. Cai, J.S. Zhang, D.Y. Tang, W.M. Cai, *China Synthetic Rubber Industry*, in press.
- [15] C.J. Tung, T.C. Hsu, *J. Appl. Polym. Sci.* 46 (1992) 1759.